

Bioinspired Synthesis of Vertically Aligned ZnO Nanorod Arrays: Toward Greener Chemistry

Lan Liu,[†] Lei Fu,[‡] Yong Liu,[†] Yaling Liu,[†] Peng Jiang,[†] Shaoqin Liu,^{*,‡} Mingyuan Gao,^{*,§} and Zhiyong Tang^{*,†}

[†]National Centre for Nanoscience and Technology, Zhongguancun Beiyitiao No. 11, Beijing 100190, P. R. China, [‡]Center for Micro and Nanotechnology, Harbin Institute of Technology, Yikuang Street No. 2, Harbin 150080, P. R. China, and [§]Institute of Chemistry, the Chinese Academy of Sciences, Zhongguancun North First Street No. 2, Beijing 100190, P. R. China

Received June 9, 2009; Revised Manuscript Received August 3, 2009

ABSTRACT: We developed a green, low-cost, bioinspired aqueous synthesis method to fabricate one-dimensional (1D) vertically aligned ZnO nanorod arrays on zinc substrates at room temperature. Scanning electron microscopy images, transmission electron microscopy images, and energy-dispersive X-ray spectrum show densely well-aligned single-crystal ZnO nanorod arrays with a length of ~400 nm fabricated by a simple method. Further, we reveal a growth mechanism that continuously deposits the freshly formed ZnO onto the zinc substrates, which results from the reaction between Zn²⁺ coordinated with cysteine and its derivatives and OH⁻ in base solution, and leads to forming ZnO nanorod arrays. More importantly, the simple preparation can grow hierarchical structures of ZnO nanorod arrays as well as fabricating the arrays on different types of zinc-based substrates. Finally, the paper reports as-prepared ZnO nanorod arrays repeatedly photobleach Rhodamine 6G, and the results suggest the photobleach efficiency increases significantly due to the arrays.

Introduction

One-dimensional (1D) vertically aligned ZnO nanorod arrays have received extensive research interest due to their potential applications in ultraviolet lasers,¹ solar energy cells,² light-emitting diodes,³ biosensors,⁴ and self-powering nanogeneration.⁵ Because of their broad application prospects, many methods and technologies have been developed to prepare 1D ZnO nanorod arrays.⁶ The first example of 1D ZnO nanoarrays is fabricated by vapor–liquid–solid (VLS) growth with either Au or Zn as the catalyst.^{1,7} However, the reaction temperature needed for this VLS technique is very high (normally around 1000 °C) to cause the excessive energy consumption. Therefore, low-temperature, solution-based methods, for example, hydrothermal and atmospheric pressure syntheses, have been explored to synthesize 1D ZnO nanorod arrays.⁸ After many improvements in synthetic conditions, 1D ZnO nanorod arrays can be produced at a low temperature of about 70 °C.⁹ Although the present synthesis methods remarkably benefit the practical applications of 1D vertically aligned ZnO nanorod arrays, more novel synthetic strategies are still desirable based on consideration of greener chemistry,¹⁰ further decreasing the reaction temperature to room temperature and using environmentally benign precursors.

Nature is our best tutor.¹¹ For example, sulfate-reducing bacterial (SRB) can simultaneously trap heavy metal ions, for example, Zn²⁺, and reduce sulfate to sulfide under ambient conditions, which subsequently leads to the formation of ZnS nanoparticle aggregates around the SRB surface.¹² Further study reveals that cysteine and cysteine-rich polypeptides or proteins on the SRB surface play a major role in trapping Zn²⁺ cations and inducing aggregation of the produced ZnS

nanoparticles.¹³ Inspired by the above discoveries, we wonder whether the amino acid cysteine may prompt the formation of ZnO nanoparticle aggregations or even 1D ZnO nanorod arrays on the substrate surface under ambient conditions, if sulfate anions in solution are replaced by hydroxyl anions.

Experimental Section

Zinc perchlorate hexahydrate (Zn(ClO₄)₂·6H₂O) and L-cysteine were purchased from Alfa Aesar. 99.99% Zn sheets, 99.99% Zn wires, and 99.99% copper sheets were purchased from Sinopharm Chemical Reagent Co. Rhodamin 6G (R6G) was purchased from Sigma. Before being used as the substrates, the commercially available Zn sheets were treated to move the oxide surface layer and became smoother by electropolishing. In the electropolishing procedure, Zn substrate was immersed in the electrolyte of alcohol and H₃PO₄ while Cu was used as a cathode.

Synthesis of 1D vertically aligned ZnO nanorod arrays: 1D ZnO nanorod arrays were prepared by immersing a zinc substrate into an equal molar aqueous solution of Zn(ClO₄)₂ (1 mM) and L-cysteine (1 mM) with a pH of 10 at room temperature for 3 days. After the reaction, the substrate was removed from the solution, ultrasonicated for 10 min, and then rinsed with deionized water before being dried in air.

Photobleaching experiments: 1D ZnO nanorod arrays grown on a zinc sheet were immersed into a 5 mL water–ethanol mixture (volume ratio of water/ethanol = 10:1) containing 0.1 mM R6G at pH 10. Subsequently, the solution was irradiated by a solar simulator (Figure S6, Supporting Information represents the spectral characteristic of the solar simulator), and the incident light intensity was 300 mW/cm². Three consecutive photobleaching experiments were performed to examine the reusability of 1D ZnO nanorod arrays. In the first experiment, 1D ZnO nanorod arrays were immersed in the R6G solution under irradiation until R6G was decreased to less than 30% compared with the original data. Then the sample of 1D ZnO nanorod arrays was picked out and washed by deionized water. In the second experiment, the above 1D ZnO nanorod arrays were immersed in a new, freshly prepared R6G solution before irradiation. The third experimental procedure was same as the second one. The serial experiments suggest 1D ZnO nanorod arrays can be reused.

*Corresponding author. Fax: (+86)10-62656765. E-mail: zytang@nanoctr.cn (Z.T.); shaoqinliu@hit.edu.cn (S.L.); gaomy@iccas.ac.cn (M.G.).

Additionally, before each photobleaching experiments, 1D ZnO nanorod arrays in R6G solution were kept in the dark for 30 min so that the R6G molecules could be adsorbed onto the surface of the nanorod arrays. UV-visible absorbance spectra of R6G were measured during the irradiation intervals. The absorbances at 525 nm in the series of spectra were applied to calculate the remaining concentration of R6G using the following equation: $100 I/I_0 = C/C_0$, where I and I_0 were the current and original absorbance peak intensities, respectively.

The morphology, crystal structure, and optical absorption of 1D vertically aligned ZnO nanorod arrays were characterized by scanning electron microscopy (Hitachi S-4800, Japan), energy-dispersive X-ray spectroscopy (EDX, Horiba), transmission electron microscopy (Tecnai G² 20 ST, America), X-ray powder diffractometer (XRD, D/max2500 Japan), and UV-vis spectra (Hitachi U-3010, Japan). The light source of photobleaching experiment was a solar simulator (PLS-SXE-300UV solar simulator, China).

Results and Discussion

The zinc substrates were immersed in the mixture solution of Zn²⁺ cations and L-cysteine (pH 10). The reason to use a base solution is to provide enough OH⁻ anions, which are necessary to produce the intermediate product of Zn(OH)₂. Since Zn(OH)₂ is thermodynamically less stable than ZnO, Zn(OH)₂ spontaneously transforms into ZnO products. After being kept in air at room temperature for a certain time,

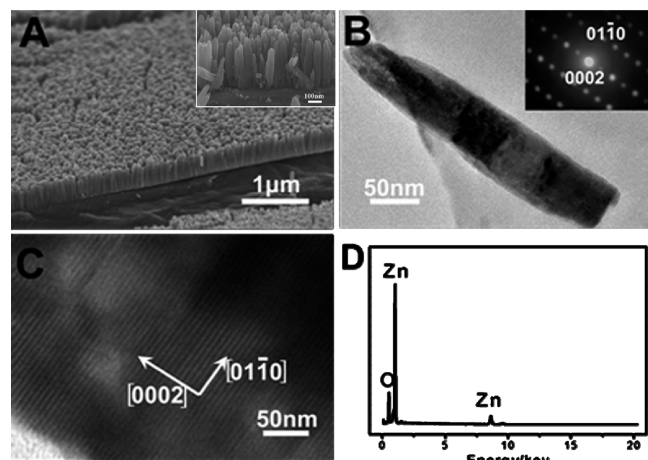


Figure 1. 1D vertically aligned ZnO nanorod arrays grown on a zinc substrate. (A) SEM image of densely aligned ZnO nanorod arrays. The inset displays the corresponding higher magnification. (B) TEM image of a single ZnO nanorod. The inset represents the selected area diffraction pattern of the nanorod. (C) HRTEM image of a single ZnO nanorod. (D) EDX spectrum of typical aligned ZnO nanorod arrays.

the zinc substrates were taken out for further characterization. Scanning electron microscopy (SEM) images confirm 1D nanorod arrays grown on a zinc substrate (Figure 1A). The high-density, vertically aligned nanorods have uniform lengths and diameters of ~400 nm and ~60 nm, respectively. Further observations from transmission electron microscopy (TEM) (Figure 1B), high-resolution TEM (HRTEM) (Figure 1C), and energy-dispersive X-ray spectroscopy (EDX) (Figure 1D) indicate that these nanorods have a single-crystalline hexagonal structure of ZnO with the growth direction along [0001].

The presence of cysteine (HSCH₂CH(COOH)NH₂) is critical for the production of 1D ZnO nanorod arrays on the zinc substrate. The contrast experiments were done with solutions that contained only Zn²⁺ cations, a mixture of Zn²⁺ cations and mercaptopropionic acid (HSCH₂CH₂COOH), or a mixture of Zn²⁺ cations and cysteamine (HSCH₂CH₂NH₂), respectively, while other experimental conditions were kept unchanged. Neither contrast experiment could create 1D ZnO nanorod arrays on the substrate (Figure S2, Supporting Information). It is known that, in base solution, Zn²⁺ cations can react with OH⁻ anions to form Zn(OH)₂, which may subsequently convert to ZnO under the long reaction time.¹⁴ The growth mode of Zn(OH)₂ or ZnO is not monotonous. When the concentration of free Zn²⁺ cations is high, Zn(OH)₂ or ZnO tends to self-nucleate in solution. On the contrary, at low concentration of free Zn²⁺ cations, the thermodynamically favorable ZnO will form and deposit on the surface of the substrate, because nucleation of a new thermodynamic phase in solution needs to overcome a high free-energy barrier. Compared with mercaptopropionic acid or cysteamine, cysteine provides three types of functional groups, thiol, carboxylic acid, and amine, which all have strong binding interactions with Zn²⁺ cations. As a result, cysteine and its derivatives can coordinate with Zn²⁺ to form polymeric network structures in solution.¹⁵ The metal-amino acid polymeric network not only lowers the concentration of free Zn²⁺ cations in solution but works as a Zn reservoir, which makes it possible for the freshly formed ZnO to continuously deposit onto the substrates. When the substrate is hexagonal zinc, the deposition and growth of hexagonal ZnO become favorable because only a 5% lattice mismatch exists between (0001)_{ZnO} and (0001)_{Zn} (0.520 vs 0.495 nm) (Figure S1, Supporting Information). Consequently, 1D ZnO nanorod arrays with the growth direction along [0001] are formed on the zinc substrates in the base solution containing Zn²⁺ and cysteine. The strong interaction between cysteine and Zn ions also explains why cysteine-rich protein can trap Zn ions and induce

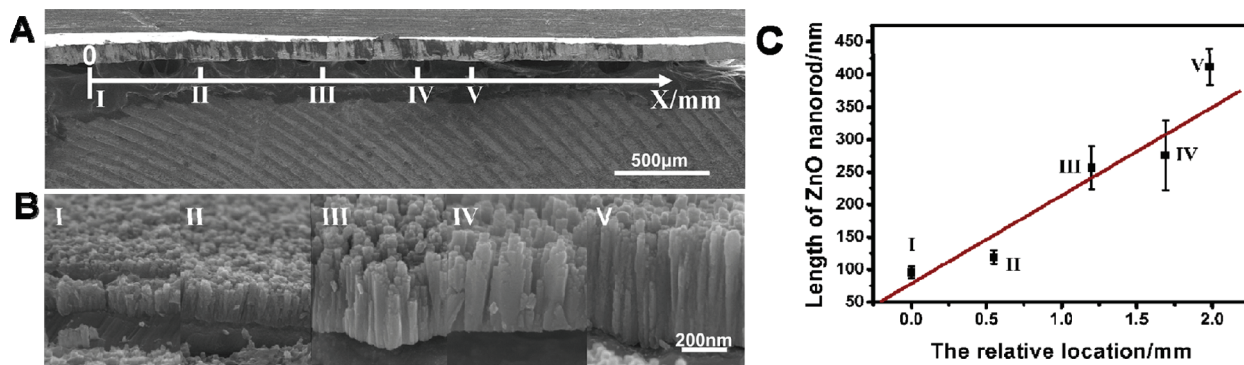


Figure 2. (A) Gradational growth of 1D ZnO nanorod arrays on the zinc substrate from left to right. (B) Cross-sectional SEM images of 1D ZnO nanorod arrays at five locations. (C) Plots of ZnO nanorod lengths against the growth positions, X.

aggregations of the produced ZnS nanoparticles on the SBR surface.¹³

The simple and easy preparation processes allow us to fabricate 1D ZnO nanorod arrays with well-controlled hierarchical structures. As an example, zinc substrates were vertically submerged in the mixture solution of Zn^{2+} and cysteine, and then they were gradually exposed to the air with natural evaporation of the solution at room temperature (the detailed preparation procedure is described in Scheme S1, Supporting Information). Zn substrate immersed in the solution was gradually exposed to the air from positions I to IV with solvent evaporation (Figure 2A), and then ZnO nanorods with different lengths were obtained (Figure 2B). To the best of our knowledge, this is the first report on templateless synthesis of the gradient nanorod arrays.¹⁶ Figure 2C shows the near-linear relationship between the

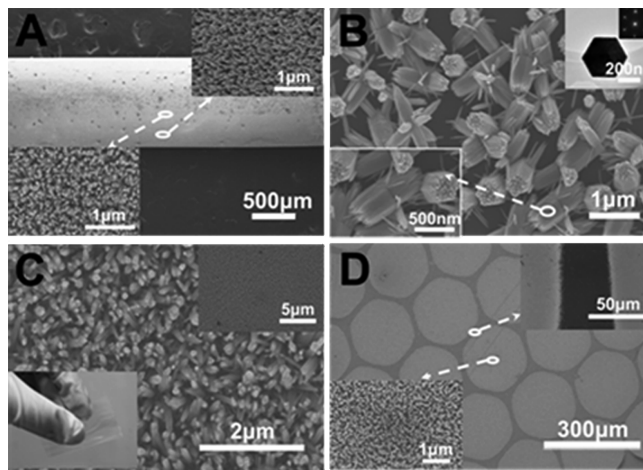


Figure 3. 1D vertically aligned ZnO nanorod arrays grown on different types of substrates. (A) Zinc wire. The insets show that 1D ZnO nanorods stand vertically on the curving surface. (B) Zn nanoplates. The upper right inset includes a TEM image and diffraction pattern of hexagonal zinc nanoplates, and the lower left inset shows a high-magnification SEM image of 1D ZnO nanorods. (C) SEM images of 1D ZnO nanorod arrays on PET substrate after bending. The upper right inset displays a large-scale image of uniform ZnO nanorod arrays on the substrate, and the left lower inset presents a bending process. (D) Pattern of 1D ZnO nanorod arrays on Si wafer. The upper right inset shows a high-magnification SEM image of the gap between two circles, and the lower left inset presents a high-magnification SEM image of the white circle.

growth lengths of ZnO nanorods and the growth positions on the substrates. We expect that such simple preparation of graded nanomaterials will open many other applications in material science and biology.¹⁶

The green preparation of 1D vertically aligned ZnO nanorod arrays is universal and can be applied to many types of the substrates with different geometries, dimensions, and properties. Figure 3 exemplifies the successful preparation of 1D vertically aligned ZnO nanorod arrays on zinc wires with the curving surface (Figure 3A), zinc nanoplates (Figure 3B), and polyethylene terephthalate (PET) plastic substrates with a thin precoated zinc layer (Figure 3C), respectively. Two interesting features of 1D ZnO nanorod arrays on the substrates should be pointed out. First, on the hexagonal zinc nanoplates of 230 nm in side-length and 10 nm in thickness, 1D ZnO nanorod arrays prefer growing on the {0001} facets rather than {0110} side facets, leading to the formation of “rod-on-plate” nanostructures (Figure 3B). The preferential growth of ZnO nanorods on {0001} facets of zinc nanoplates is reasonable due to the small lattice mismatch of $(0001)_{ZnO}/(0001)_{Zn}$. Second, the 1D ZnO nanorod arrays, which are grown on the PET plastic substrates precoated with a zinc thin film, can remain the array structures even after many cycles of mechanic bending (Figure 3C and Figure S5, Supporting Information). The good mechanical tolerance of 1D ZnO nanorod arrays on PET substrates suggests potential applications in plastic-based devices. Moreover, selective growth of 1D ZnO nanorod arrays is also realized by immersion of silicon substrates, whose surfaces are precoated with zinc patterns, in the mixture solution of Zn^{2+} and cysteine. Figure 3D reveals that ZnO nanorod arrays are exclusively grown on the zinc microcircles (the inset in the lower left corner) instead of bare silicon gaps (the inset in the upper right corner). Such selective growth of ZnO nanorods can be also explained by a good lattice match of $(0001)_{ZnO}/(0001)_{Zn}$.

The application of as-synthesized 1D ZnO nanorod arrays in photobleaching of organic dyes was preliminarily examined.¹⁷ The ZnO nanorod arrays with a length of ~ 400 nm were put in the water–ethanol mixture containing R6G. The water–ethanol mixture was used to assist the separation of electron–hole pairs generated by ZnO nanorod arrays under the irritation of a solar simulator. The photo-generated holes were captured by ethanol, and simultaneously the photogenerated electrons reduced the organic dye R6G in solution. Figure 4A shows UV–visible absorption spectra of

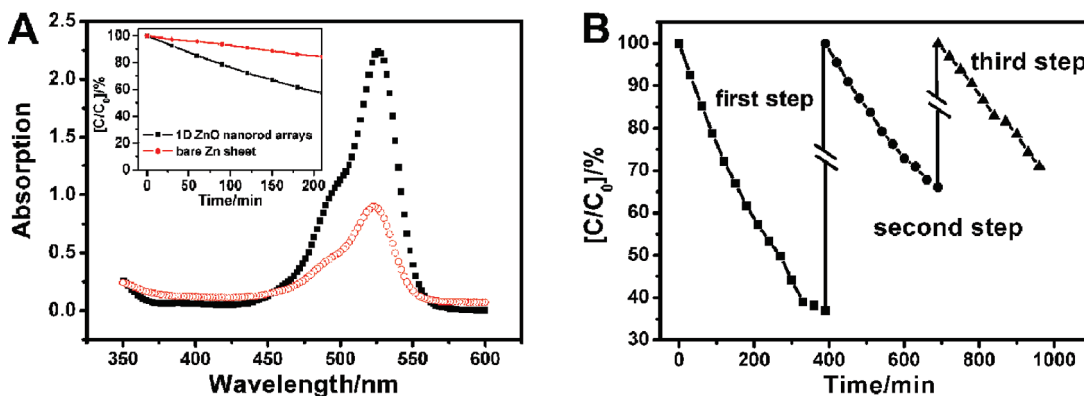


Figure 4. (A) UV–visible absorption spectra of R6G before (■) and after (○) 3.5 h photobleaching by using 1D ZnO nanorod arrays. The inset shows the relationship between the concentration of the remaining R6G and the photobleaching time, and here C_0 and C are initial and real concentrations of R6G calculated from their absorbance peaks at 525 nm, respectively. (B) Relationship between the remaining concentration of R6G and the photobleaching time from three cycles of experiments.

R6G by using ZnO nanorod arrays before and after 3.5 h irradiation. Compared with bare zinc substrates (the slight photobleaching may originate from the formed ZnO particles during the experiments, Figure S7), 1D ZnO nanorod arrays exhibit much faster photobleaching rates against R6G (inset in Figure 4A). This result proves the photobleaching function of ZnO nanorod arrays to organic dyes.¹⁸ The unique advantage of ZnO nanorod arrays is their easy collection property from solution, which makes them reusable in photobleaching of organic dyes. Figure 4B shows three consecutive photobleaching experimental results by using the same ZnO nanorod arrays. Although photobleaching rates of R6G at the following cycles are slightly slower than that at the first cycle (Figure 4B) and the ZnO structure is partially changed after three cycles (Figure S8), ZnO nanorod arrays still remain high efficiency against photobleaching of organic dyes.

Conclusion

In summary, inspired by the nanomanufacturing behaviors of sulfate-reducing bacteria, we developed a novel method to synthesize 1D vertically aligned ZnO nanorod arrays in the mixture solution of amino acid cysteine and Zn²⁺ cations at room temperature. The environmentally friendly method can prepare 1D ZnO nanorod arrays with hierarchical structures on different zinc-based substrates with varying shapes, dimensions, and patterns. The formation mechanism of 1D ZnO nanorod arrays on the zinc substrates are ascribed to the polymeric network structures of Zn-cysteine in solution, which effectively prevents possible self-nucleation of ZnO in solution and meanwhile promotes deposition of ZnO onto the substrates. The low-cost, green synthesis method may open many applications of 1D vertically aligned ZnO nanorod arrays in different fields, for example, water treatment or plastic devices.

Acknowledgment. The authors thank the National High-tech Research and Development Program (2007AA03Z302, Z.Y.T., S.Q.L.), 100-talent program of Chinese Academy of Sciences (Z.Y.T.), Start-up funding of HIT (S.Q.L.), the National Science Foundation of China (20773033, Z.Y.T.), and the National Research Fund for Fundamental Key Project (2009CB930401, Z.Y.T.) for financial support of this research.

Supporting Information Available: Detailed experimental section, XRD data, SEM images obtained by immersing Zn substrates into the solutions and different zinc-based substrates and ZnO film before and after the bending process, the spectrum of the solar simulator, SEM image and EDX data of blank Zn plates after photobleaching experiments and SEM image of ZnO nanorod arrays after three cycles of photobleaching experiments. This information is available free of charge via the Internet at <http://pubs.acs.org/>.

References

- Huang, M. H.; Mao, S.; Feick, H.; Yan, H. Q.; Wu, Y. Y.; Kind, H.; Weber, E.; Russo, R.; Yang, P. D. *Science* **2001**, *292*, 1897–1899.
- Law, M.; Greene, L. E.; Johnson, J. C.; Saykally, R.; Yang, P. D. *Nat. Mater.* **2005**, *4*, 455–459.
- Park, W. I.; Yi, G.-C. *Adv. Mater.* **2004**, *16*, 87–90.
- Wei, A.; Sun, X. W.; Wang, J. X.; Lei, Y.; Cai, X. P.; Li, C. M.; Dong, Z. L.; Huang, W. *Appl. Phys. Lett.* **2006**, *89*, 123902.
- Qin, Y.; Wang, X. D.; Wang, Z. L. *Nature* **2008**, *451*, 809–813.
- Wang, Z. L. *Mater. Sci. Eng., R* **2009**, *64*, 33–71.
- Wang, X.; Summers, C. J.; Wang, Z. L. *Nano Lett.* **2004**, *4*, 423–426.
- Vayssières, L. *Adv. Mater.* **2003**, *15*, 464–466.
- Xu, S.; Wei, Y. G.; Kirkham, M.; Liu, J.; Mai, W. J.; Davidovic, D.; Snyder, R. L.; Wang, Z. L. *J. Am. Chem. Soc.* **2008**, *130*, 14958–14959.
- Dahl, J. A.; Maddux, B. L. S.; Hutchison, J. E. *Chem. Rev.* **2007**, *107*, 2228–2269.
- Dickerson, M. B.; Sandhage, K. H.; Naik, R. R. *Chem. Rev.* **2008**, *108*, 4935–4978.
- (a) Labrenz, M.; Druschel, G. K.; Ebert, T. T.; Gilbert, B.; Welch, S. A.; Kemner, K. M.; Logan, G. A.; Summons, R. E.; Stasio, G. D.; Bond, P. L.; Lai, B.; Kelly, S. D.; Banfield, J. F. *Science* **2000**, *290*, 1744–1747. (b) Moreau, J. W.; Webb, R. I.; Banfield, J. F. *Am. Mineral.* **2004**, *89*, 950–960.
- Moreau, J. W.; Weber, P. K.; Martin, M. C.; Gilbert, B.; Hutcheon, L. D.; Banfield, J. F. *Science* **2007**, *316*, 1600–1603.
- Zhang, H.; Yang, D.; Ji, Y. J.; Ma, X. Y.; Xu, J.; Que, D. L. *J. Phys. Chem. B* **2004**, *108*, 3955–3958.
- (a) Rebilly, J. N.; Gardner, P. W.; Darling, G. R.; Bacsa, J.; Rosseinsky, M. J. *Inorg. Chem.* **2008**, *47*, 9390–9399. (b) Fischer, K. *Water, Air, Soil Pollut.* **2002**, *137*, 267–286. (c) Gocke, P.; Vogler, R.; Gelinsky, M.; Meissner, A.; Albrich, H.; Vahrenkamp, H. *Inorg. Chim. Acta* **2001**, *323*, 16–22. (d) Chen, Z. L.; Su, Y.; Xiong, W.; Wang, L. X.; Liang, F. P.; Shao, M. *CrystEngComm* **2009**, *11*, 318–328.
- Sehayek, T. L.; Vaskevich, A.; Rubinstein, I. *J. Am. Chem. Soc.* **2003**, *125*, 4718–4719.
- Maeda, K.; Takata, T.; Hara, M.; Saito, N.; Inoue, Y.; Kobayashi, H.; Domen, K. *J. Am. Chem. Soc.* **2005**, *127*, 8286–8287.
- Mansoori, R. A.; Kothari, S.; Ameta, R. *Arabian J. Sci. Eng.* **2004**, *29*, 11–16.